

Aligned ZnO Nanorod@Ni-Co Layered Double Hydroxide Composite Nanosheets Arrays with Core-Shell Structure as High- Performance Supercapacitor Electrode Materials

Xiaojuan Liu, Hao Liu, Xinzhi Sun*

College of Chemistry and Pharmaceutical Sciences, Qingdao Agricultural University,

Qingdao 266109, China

*Corresponding author: Tel/Fax: 86-532-86080855;

E-mail: xzsun@qau.edu.cn

Experimental

2.1. Chemical and materials

All the chemicals were of analytical grade and used without further purification.

Zinc nitrate hexahydrate ($\text{Zn}(\text{NO}_3)_2 \cdot 6\text{H}_2\text{O}$, 99% purity, Sigma), hexamethylenetetramine (HMTA, 99%, National Medicine Co.), ammonia ($\text{NH}_3 \cdot \text{H}_2\text{O}$, 25 wt%, National Medicine Co.).

2.2. Electrochemical measurements for three-electrode systems

The electrochemical performances of the single electrode were studied under a standard three-electrode system. The ZnO NRAs, Ni-Co LDH NSs and ZnO NR@Ni-Co LDH CNSAs on carbon cloth were all served as the working electrode, Pt wire as the counter electrode, and a saturated calomel electrode (SCE) as reference electrode, respectively. Cyclic voltammetry (CV), galvanostatic charge-discharge (GCD), and electrochemical impedance spectroscopy (EIS) measurement were carried out on CHI 660E electrochemical station (CHI, Shanghai, Chenhua Co.) at room temperature. CV was conducted at different scan rates to determine the electrochemical properties in 2 mol L⁻¹ KOH solution. A series of the cyclic voltammograms (CVs) were obtained in the working potential between 0 and 0.9 V vs SCE at the different scan rates of 10, 20, 40, 50, 60, 80, and 100 mV s⁻¹. GCD tests were carried at the working potential between 0 and 0.9 V vs SCE at the various current densities of 1, 2, 3, 4, 5, 6, 8 and 10 A g⁻¹, respectively. EIS was carried out under a sinusoidal signal over a frequency range from 1-10⁵ Hz with a magnitude of 10 mV.

The specific capacitance of the electrode and the device were calculated by using above-mentioned GCD curves at different current densities according to the following equations:

$$C = \frac{I \cdot \Delta t}{m \cdot \Delta V}$$

Where I (A) is the charge or discharge current, Δt (s) is the discharge time, m (g) is the mass of electroactive materials in the working electrode, and ΔV (V) is the potential window (obtained from the discharge curves excluding the potential drop).

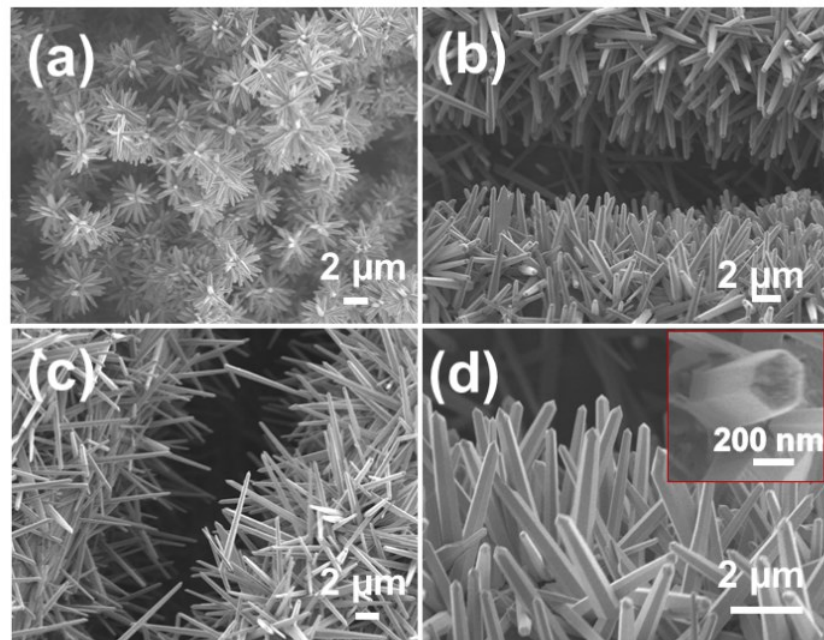


Fig. S1 SEM images of ZnO NRs with different concentration of $Zn(NO_3)_2$ solution (a) 1.8mM (b) 2.7mM (c) 3.6 mM (d) the high magnification of (c) and the inset is enlarged of a ZnO NR

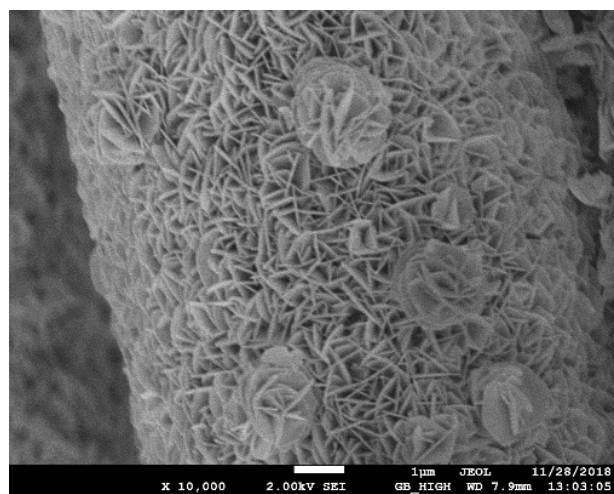


Fig. S2 SEM image of Ni-Co LDH nanosheets

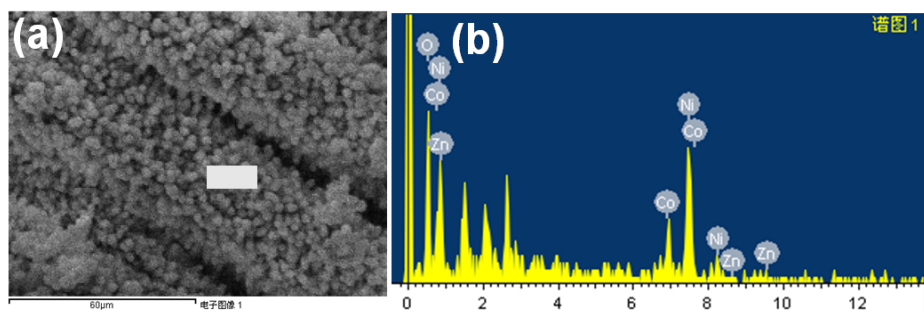


Figure S3 SEM images and the EDX spectra of ZnO NR@Ni-Co CNSs

Table S1 Elemental distribution of ZnO NR@Ni-Co CNSs

Element	O	Co	Ni	Zn
Weight (%)	17.83	17.94	61.34	2.89
Atom (%)	44.43	12.14	41.67	1.76

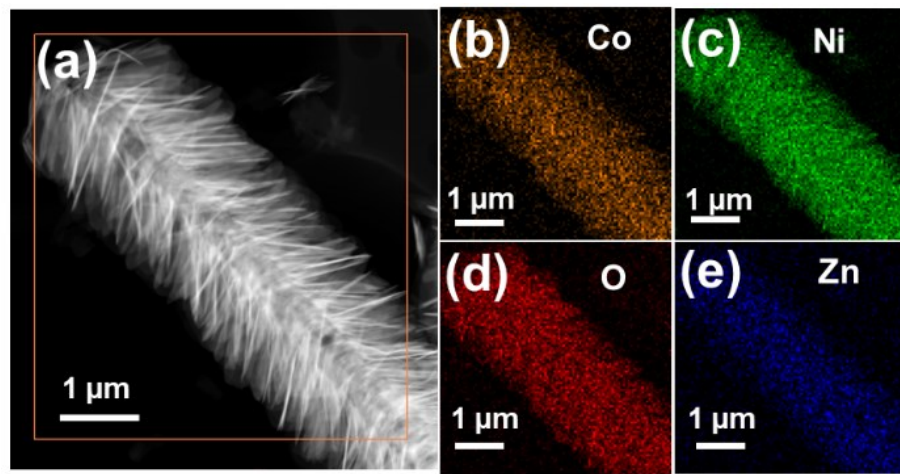


Fig. S4 The elemental mapping of ZnO NR@Ni-Co CNSs. (a) TEM image of an individual ZnO NR@Ni-Co CNS and elemental mapping of Co (b), Ni (c), O (d), and Zn (e)

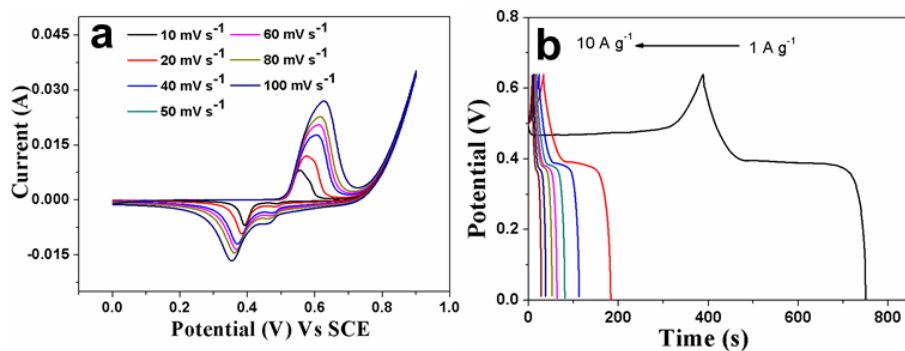


Fig. S5 (a) CV curves of Ni-Co LDH NSs at different scan rates and (b) GCD curves of Ni-Co LDH NSs at different current densities

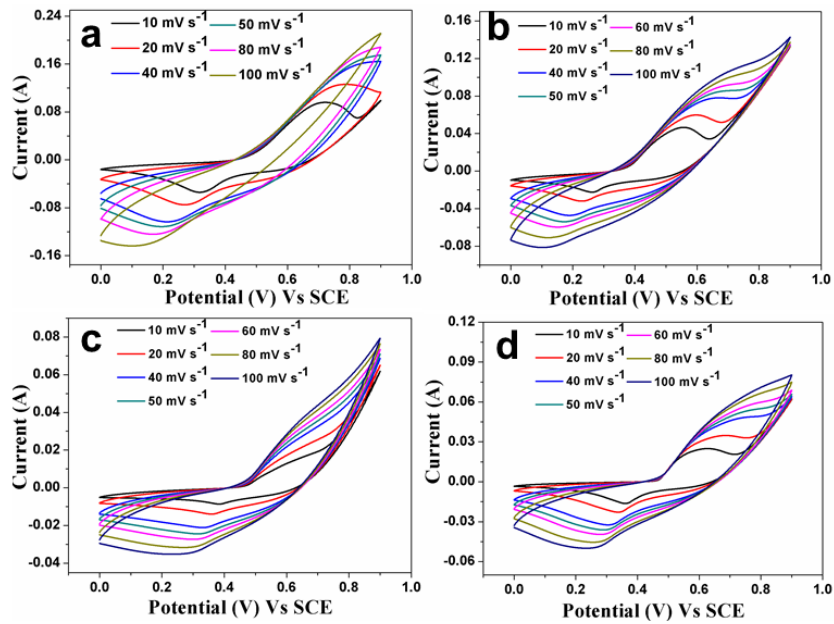


Fig. S6 CV curves of ZnO NR@Ni-Co LDH CNSAs prepared under different reaction time (a) 3 h, (b) 12 h, (c) 18 h, (d) 24 h at different scan rates.

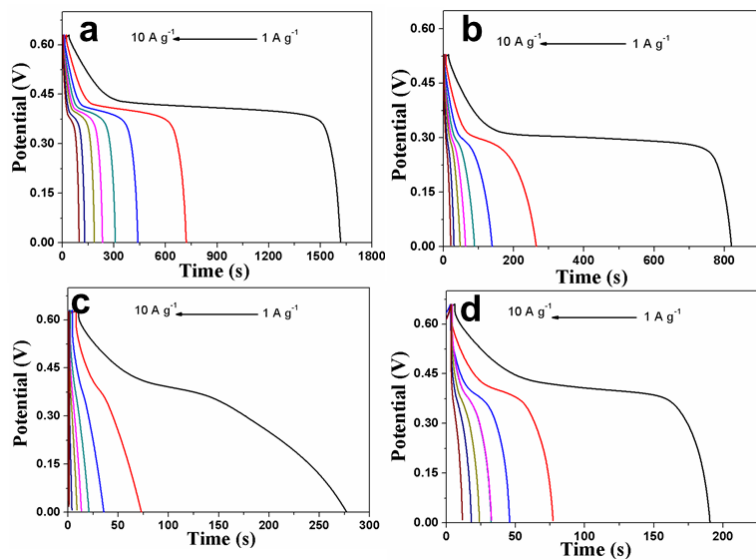


Fig. S7 GCD curves of the ZnO NR@Ni-Co LDH CNSAs prepared under different reaction time, (a) 3 h, (b) 12 h, (c) 18 h, (d) 24 h at different current densities.

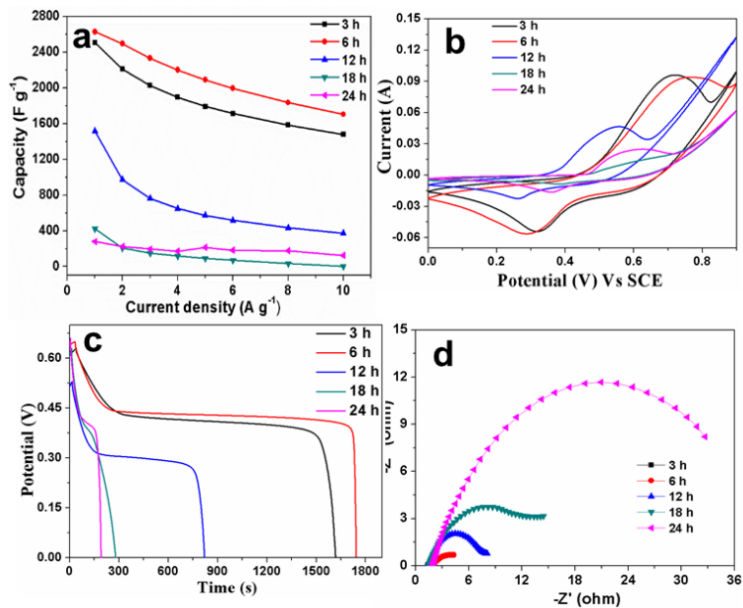


Fig. S8 Comparison of (a) specific capacitance as a function of current density, CV curves (b), GCD curves (c) and Nyquist plots (d) of ZnO NR@Ni-Co LDH CNSAs prepared at different reaction time

Table S2 Comparison of the maximum Cs with the different electrode materials based on nickel and/or cobalt composites

Electrode materials	Current density	Specific capacitance	Ref.
CoNi(OH) ₂ /graphene	0.5	2360	S1
Ni-Co oxide nano-composite	0.2	287	S2
NiCo ₂ O ₄ /carbon fiber	1	1422	S3
Nanostructured NiCo ₂ O ₄ spinel	1	671	S4
NiCo LDH/RGO	2	1911.1	S5
Nickel cobaltite nanowire	1	760	S6
Porous Ni(OH) ₂ /NiOOH composite	2	1420	S7
Co ₃ O ₄ /NiO nanowire arrays	2	853	S8
Doughnut-like Ni(OH) ₂ -Co(OH) ₂ composite	2	2191	S9
Nickel cobalt LDHs/Zn ₂ SnO ₄	0.5	2193	S10
NiCo ₂ S ₄ ball-in-ball hollow spheres	1	1036	S11
Ni-Co LDH@diamite@NF	1	514	S12
ZnO NR@Ni-Co LDH CNSAs	1	2683.8	This work

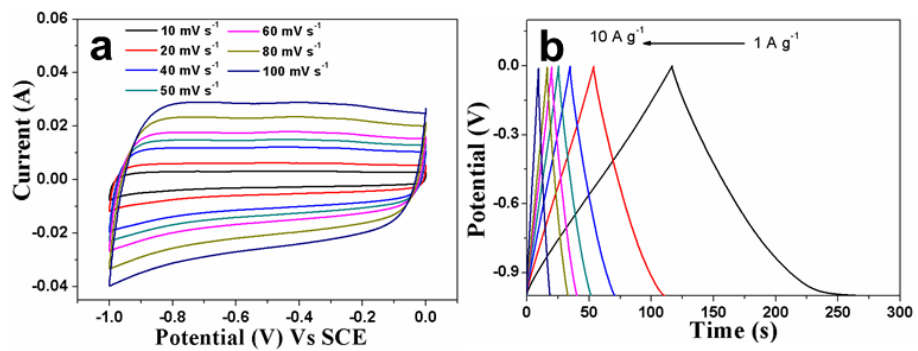


Fig. S9 CV curves at the different scan rate and GCD curves at the different current density of AC

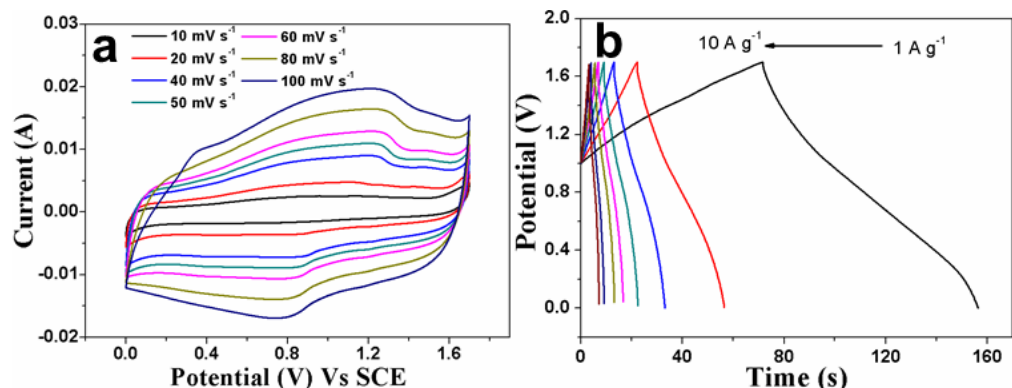


Fig. S10 CV curves at the different scan rate and GCD curves at the different current density of Ni-Co LDH NSs//AC

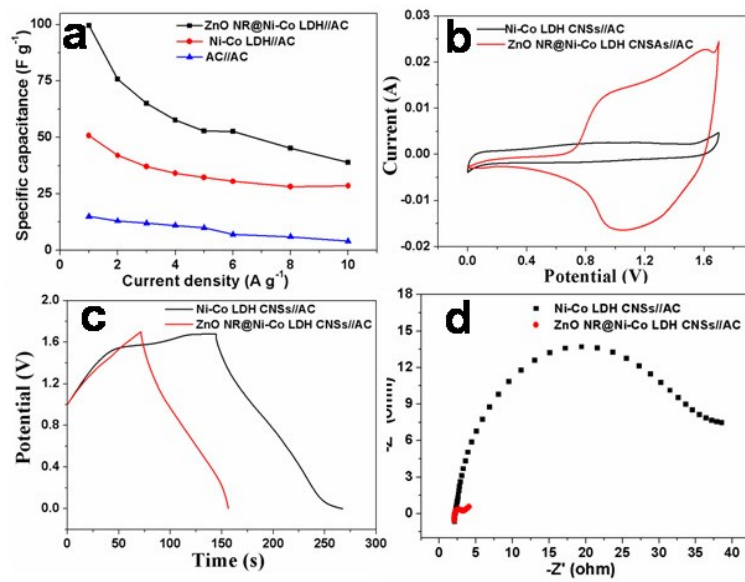


Fig. S11 (a)The specific capacitance of ZnO NR@Ni-Co LDH CNSAs//AC, Ni-Co LDH NSs//AC and AC//AC devices calculated based on the galvanostatic discharge curves as a function of the current densities, comparison of CV curves (b), GCD curves(c) and EIS (d) of ZnO NR@Ni-Co LDH CNSAs//AC and Ni-Co LDH NSs//AC

Table S3 Comparison of the maximum energy densities, corresponding average power density based on active materials and potential window of some reported nickel or cobalt oxide/hydroxide based asymmetric supercapacitors

Positive materials//negative materials	Energy density (Wh kg ⁻¹)	Power density (Kw kg ⁻¹)	Potential window (V)	Ref.
Ni-Co oxide//AC	12.0	0.1	0-1.2	S13
Graphitic carbon spheres-MnO ₂	22.1	0.10	0-2.0	S14
nanofibers//graphitic carbon spheres				
Nickel cobalt LDHs//AC	23.7	0.28	0-1.2	S10
Co _{0.45} Ni _{0.55} O/RGO//RGO	35.3	0.33	0-1.5	S15
RGO-CoAl LDH//AC	35.5	0.875	0-1.75	S16
NiCo ₂ O ₄ @MnO ₂ //AC	35	0.163	0-1.5	S17
Graphite oxide-MnO ₂ //graphite oxide	24.3	24.5 (P _{max})	0-2.0	S18
Ni _x Co _{1-x} O//AC	37.4	0.163	0-1.6	S19
Ni(OH) ₂ -MnO ₂ -RGO//FRGO	32.6	0.31	0-1.6	S20
CoMoO ₄ @3D graphene//AC	21.1	0.3	0-1.8	S21
CoAl-LDHs/CNTs//AC	28	0.444	0-1.6	S22
MnO ₂ //graphene	25.2	0.10	0-2.0	S23
AC//β-Ni(OH) ₂ /Ni-foam	36.2	0.100	0-1.8	S24
MnO ₂ nanowire-SWCNT//In ₂ O ₃	25.5	50.3 (P _{max})	0-2.0	S25
nanowire SWCNT				
Poly(3,4-ethylenedioxythiophene)-	30.2	0.18	0-1.8	S26
MnO ₂ //AC				
ZnO NR@Ni-Co LDH CNSAs//AC	40.4	1.118	0-1.7	This work



Fig. S12 The photograph of 16 commercial red LEDs powered by two as-prepared ASC in series

Reference:

- [S1] Y. Cheng, H. Zhang, C.V. Varanasi, J. Liu, *Energy. Environ. Sci.*, 2013, 6, 3314-3321.
- [S2] J.J. Deng, J.C. Deng, Z.L. Liu, H.R. Deng, B. Liu, *J. Mater. Sci.*, 2009, 44, 2828-2835.
- [S3] F. Deng, L. Yu, G. Cheng, T. Lin, M. Sun, F. Ye, Y. Li, *J. Power Sources*, 2014, 251, 202-207.
- [S4] C. Wang, X. Zhang, D. Zhang, C. Yao, Y. Ma, *Electrochimica Acta*, 2012, 63, 220-227.
- [S5] X. Cai, X. Shen, L. Ma, Z. Ji, C. Xu, A. Yuan, *Chemical Engineering Journal*, 2015, 268, 251-259.
- [S6] H. Wang, Q. Gao, L. Jiang, *Small*, 2011, 7, 2454-2459.
- [S7] Y. F. Yuan, X. H. Xia, J. B. Wu, J. L. Yang, Y. B. Chen, S. Y. Guo, *Electrochimica Acta*, 2011, 56, 2627-2632.
- [S8] X. Xia, J. Tu, Y. Zhang, X. Wang, C. Gu, X. Zhao, H.J. Fan, *ACS nano*, 2012, 6, 5531-5538.
- [S9] J. Li, M. Yang, J. Wei, Z. Zhou, *Nanoscale*, 2012, 4, 4498-4503.
- [S10] X. Wang, A. Sumboja, M. Lin, J. Yan, P. S. Lee, *Nanoscale*, 2012, 4, 7266-7272.
- [S11] L. Shen, L. Yu, H. B. Wu, X. Yu, X. Zhang, X. W. Lou, *Nat. Comm.*, 2015, 6, 6694(1-8).
- [S12] Jing C, Liu X, Liu X, et al. CrystEngComm, 2018, 20(46): 7428-7434.
- [S13] C. Tang, Z. Tang, H. Gong, *J. Electrochem. Soc.*, 2012, 159, A651-A656.
- [S14] Z. Lei, J. Zhang, X.S. Zhao, *J. Mater. Chem.*, 2012, 22, 153-160.
- [S15] J. Xiao, S. Yang, *J. Mater. Chem.*, 2012, 22, 12253-12262.
- [S16] W. Zhang, C. Ma, J. Fang, J. Cheng, X. Zhang, S. Dong, L. Zhang, *RSC Advances*, 2013, 3, 2483-2490.

- [S17] K. Xu, W. Li, Q. Liu, B. Li, X. Liu, L. An, Z. Chen, R. Zou, J. Hu, *J. Mater. Chem. A*, 2014, 2, 4795-4802.
- [S18] X. Zhao, L. Zhang, S. Murali, M.D. Stoller, Q. Zhang, Y. Zhu, R.S. Ruoff, *ACS Nano*, 2012, 6, 5404-5412.
- [S19] X. Wang, C. Yan, A. Sumboja, P. S. Lee, *Nano Energy*, 2014, 3, 119-126.
- [S20] H. Chen, S. Zhou, L. Wu, *ACS Appl. Mater. Interfaces*, 2014, 6, 8621-8630.
- [S21] X. Yu, B. Lu, Z. Xu, *Adv. Mater.*, 2014, 26, 1044-1051.
- [S22] L. Yu, N. Shi, Q. Liu, J. Wang, B. Yang, B. Wang, H. Yan, Y. Sun, X. Jing, *Phys. Chem. Chem. Phys.*, 2014, 16, 17936-17942.
- [S23] Cao, J. Wang, Y. Zhou, Y. Ouyang, J.H. Jia, D. Guo, L. *J. Electroanal. Chem.*, 2013, 689, 201-206.
- [S24]. P.C. Chen, G. Shen, Y. Shi, H. Chen, C. Zhou, *ACS Nano*, 2010, 4, 4403-4411.
- [S25]. Y. Cheng, H. Zhang, S. Lu, C.V. Varanasi, J. Liu, *Nanoscale*, 2013, 5, 1067-1073.
- [S26]. Tang, P.; Zhao, Y.; Xu, C. *Electrochimica Acta*, 2013, 89, 300-309.